Journal of Catalysis **207,** 353–360 (2002)
doi:10.1006/jcat.2002.3533, available online at http://www.idealibrary.com on IDEAL®

Modification of the Acidic Properties of NaY Zeolite by H_2S Adsorption—An Infrared Study

Françoise Maugé,*,[1] Abdelaziz Sahibed-Dine,*,† Marina Gaillard,* and Maria Ziolek‡

*Laboratory "Catalyse et Spectrochimie," UMR CNRS 6506, ISMRA, University of Caen, 14050 Caen Cedex, France; †Faculty of Sciences, Chouaib Doukkali University, El Jadida, Morocco; and ‡Faculty of Chemistry, A. Mickiewicz University, Grunwaldzka 6, 60-580 Poznan, Poland

Received October 18, 2001; revised December 28, 2001; accepted December 28, 2001

The modification of acidic properties resulting from H_2S adsorption on the NaY zeolite were studied by IR spectroscopy using pyridine and 2,6-dimethylpyridine as probe molecules. A very small fraction of H_2S adsorbs dissociatively on NaY whereas the main part of H_2S interacts nondissociatively, either by coordination with Na^+ cations or by H-bonding. Evacuation at room temperature (RT) eliminates all the molecular H_2S species. Both probe molecules detected Brønsted acidity in the presence of H_2S but this acidity is almost completely eliminated by pumping at RT. No link between the variation in the number of protonated species and the variation in the intensity of the OH bands appears. On the contrary, there is a relationship between the presence of molecular H_2S and the detection of protonated species. These results show that coordination of H_2S on cationic sites leads to a modification of the electronic repartition in the hydrogen disulfide molecule, giving rise to the appearance of a positive charge on the hydrogen atom of the molecular H_2S, which, thus, presents a proton-donating ability.

INTRODUCTION

The more-severe environmental legislations lead the industry to provide fuels with a lower sulfur content to reduce sulfur emission. Therefore, there is a need to go further in the investigation of catalysts for sulfur elimination and transformation processes, such as hydrotreatment, hydrocracking, and Claus reaction. Improvement in knowledge of the surface sites of these catalysts requires characterization under conditions closer to the reaction conditions, particularly in the presence of hydrogen sulfide.

Indeed, it is worth noting that modification of the catalyst surface via the chemisorption of hydrogen sulfide occurs in catalytic processes in which H_2S plays the role of reactant. The reactions mainly require the presence of basic centers on the catalytic surface, such as the Claus and Super Claus processes (1), or the hydrosulfurization of alcohols (2–5) and the transformation of other oxo-organic compounds into sulfur-containing ones (6, 7). In the reactions mentioned above, the chemisorption of hydrogen sulfide can modify the catalyst properties during the time-on-stream and it can change the activity and/or selectivity of the process. Therefore, knowledge of the nature of the catalyst surface after the chemisorption of H_2S is very important.

For hydrotreatment, previous studies reported also the sensitivity of the surface properties of the catalyst to the presence of H_2S, a product of the hydrodesulfurization (HDS) reaction (8). Spectroscopic studies showed that acidic properties of the HDS catalyst are transformed in the presence of hydrogen sulfide. Indeed, dissociative adsorption of H_2S occurs on the sulfide phase as well as on the alumina support and leads to a decrease in the number of coordinative unsaturated sites (CUS) and to the creation of Brønsted acid sites (9, 10). Additionally, in a recent study, we observed that the molecular adsorption form of H_2S can also perturb the acid base properties of the catalyst (11). To go further in the understanding of this feature, we chose as adsorbent a well-defined catalyst where H_2S mainly adsorbs nondissociatively (12). Therefore, we extended the previous study to the characterization of the effect of H_2S adsorption on the acidic properties of a Y zeolite. Such a catalyst presents also the advantage of being able to be used as support for hydrocracking catalysts.

Adsorption of H_2S on zeolites has already been the subject of several papers (for example, 12–15). However, few studies have been concerned with the modifications of the acidic properties induced by H_2S adsorption. Karge and Rasko (12) investigated H_2S adsorption on a faujasite-type zeolite with various Si/Al ratios. Their results showed that on NaX zeolite H_2S adsorbs dissociatively, leading to the creation of OH groups and SH groups, with the latter being characterized by a ν(SH) band at 2560 cm^{-1}. With increasing pressure of H_2S, IR spectroscopy shows that the SH band broadens and shifts toward lower wavenumbers. The new OH groups or at least a part of them exhibit Brønsted acidity. In contrast, on the NaY zeolite, H_2S adsorbs almost without dissociation. The authors did not observe any Brønsted acidity when H_2S was adsorbed on NaY zeolite. In a more recent study, Karge *et al.* (13) proposed, from

[1] To whom correspondence should be addressed. Fax: +33(0)2.31.45.28.22. E-mail: Francoise.Mauge@ismra.fr.

0021-9517/02 $35.00

IR and UV–visible (UV–vis) spectroscopic results, that on sodium X and Y zeolites, for the first H_2S doses, a complete dissociation of H_2S could occur, leading to the formation of $2H^+$ and S^{2-}. Forster and Schuldt (14) studied H_2S adsorption on A zeolites exchanged with various alkaline cations. These authors showed that H_2S preferential adsorption depends on the nature of the countercations and of the exchange level. Hosotsubo *et al.* (15) have studied the influence of H_2S on the catalytic activities of a wide range of metal ion-exchanged Y zeolites for several acid-catalyzed reactions, such as cumene cracking, toluene disproportionation, and *o*-xylene isomerization and disproportionation. From infrared data, it was concluded that the increase in the catalytic activity observed after H_2S treatment is a result of the formation of new OH groups acting as Brønsted acid sites.

In a first approach, we chose, as starting material, a pure NaY sample, i.e., a zeolite that initially does not contain any Brønsted acidity. Acidic properties were characterized by IR spectroscopy, using two kinds of probe molecules: pyridine and 2.6-dimethylpyridine (lutidine, DMP), with the latter being more sensitive to weak Brønsted acidity than pyridine due to its greater basicity (16). DMP as well as pyridine gives rise to bands characteristic of the various modes of interaction of the probe with the surface (17–19). As for DMP adsorption, the 1660- to 1580-cm^{-1} region is particularly interesting due to the occurrence of bands of ν_{8a} and ν_{8b} vibrations, the most sensitive to the DMP adsorption mode. Indeed, the bands between 1618 and 1580 cm^{-1} are due to coordinated DMP or weakly adsorbed DMP, whereas those between 1655 and 1625 cm^{-1} correspond to protonated DMP ($DMPH^+$).

EXPERIMENTAL

The studied catalyst was a commercial sodium Y zeolite provided by Union Carbide, whose formula is $Na_{54}(AlO)_{54}(SiO)_{138}$.

The catalyst was pressed into a self-supported disk ($5\ mg \cdot cm^{-2}$) and activated *in situ* in a quartz IR cell. These pretreatment conditions were chosen in order to avoid dealumination of the zeolite and extraframework formation. The zeolite was heated under evacuation up to 523 K at a rate of $2\ K \cdot min^{-1}$ and evacuated for 2 h at this temperature. Then, the temperature was increased to 673 K at a rate of $1.25\ K \cdot min^{-1}$ and the catalyst was maintained for 9 h at this temperature under dynamic vacuum. Finally, the catalyst temperature was decreased to room temperature (RT). At the end of the activation, the residual pressure in the IR cell was $P \sim 2 \times 10^{-6}$ bars.

Before introduction of the H_2S (Air Liquide, 1.1% COS as main impurities) in the IR cell, the hydrogen disulfide was submitted to cryogenic trapping to remove traces of water. Then, successive doses of H_2S were introduced into the IR cell (8, 25, 70, 150, 320, 740, and 1580 μmol per g of catalyst). H_2S was further evacuated at RT. In this paper, the zeolite contacted with the various H_2S doses is denoted NaY*xx*, where *xx* corresponds to the total number of micromoles per gram of H_2S catalyst introduced.

The acidic properties of the catalyst were tested by adsorption of the basic molecules pyridine or 2,6-dimethylpyridine (DMP, lutidine) at RT. To characterize the modification of acidic properties induced by the H_2S adsorption, the probe molecules were adsorbed before or after addition of H_2S ($1580\ \mu mol \cdot g^{-1}$). The catalyst was contacted either directly with 3 Torr at equilibrium of the probe or with calibrated doses (40, 125, or 250 μmol of probe per g of catalyst) successively introduced into the IR cell and, finally, with 3 Torr at equilibrium. The catalyst was then evacuated.

RESULTS AND DISCUSSION

Effect of H_2S Adsorption

In a first step, surface sites of the NaY zeolite were characterized in the absence and in the presence of H_2S without adsorption of the basic probe molecule.

In the 4000- to 3500-cm^{-1} zone, the IR spectrum of the catalyst evacuated at 673 K presents only a very small band at 3745 cm^{-1} (Fig. 1). This band is characteristic of isolated SiOH groups, indicating the presence of a small number of defects in the studied zeolite. Moreover, the absence of any ν(OH) bands at ~3650 and ~3550 cm^{-1}, which are characteristic of hydroxyl groups of the supercage (OH(HF)) and of the sodalite cages (OH(LF)) of the Y zeolite, confirms that the initial zeolite is a pure cationic (sodium) form, as indicated by the chemical composition. In the low-frequency zone, three IR bands are observed, at 1890, 1765, and 1640 cm^{-1}, which correspond to the harmonic of structural Al–O and Si–O vibrations (Fig. 1).

The effect of H_2S introduction into the NaY sample is presented by the spectra shown in Fig. 2. Important modifications of the surface species can be noted. In the 4000- to

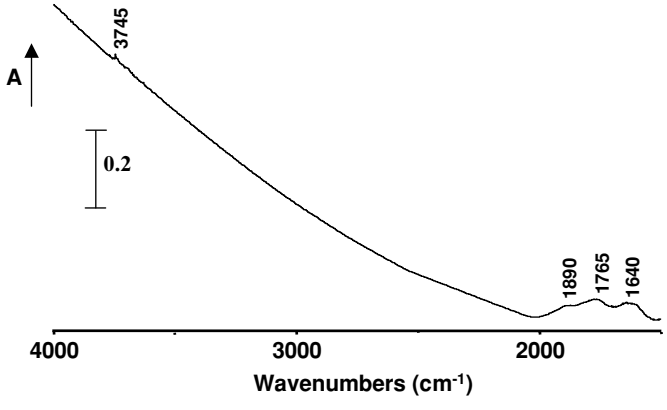

FIG. 1. IR spectrum of NaY zeolite evacuated at 673 K for 9 h.

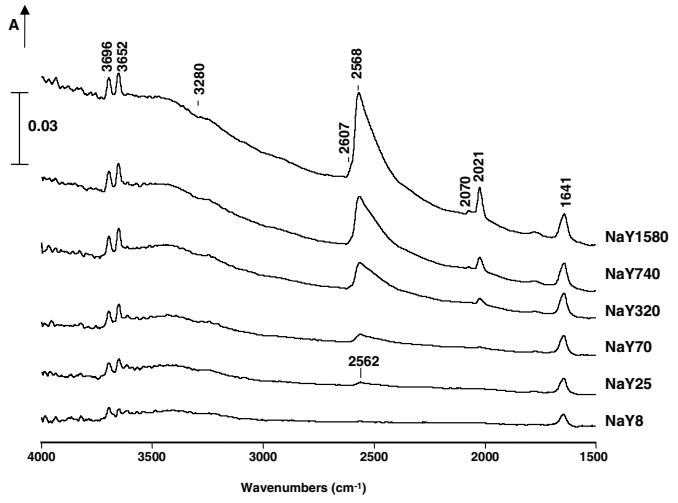

FIG. 2. IR spectra after the adsorption of increasing doses of H_2S on NaY zeolite: 8, 25, 70, 320, 740, and 1580 μmol per g of catalyst (difference spectra: after H_2S adsorption minus before).

3500-cm^{-1} zone, as soon as H_2S is introduced, two bands, at 3696 and 3652 cm^{-1}, are created. The maximum intensity of the band at 3696 cm^{-1} is observed for NaY70 while the intensity of the OH band at 3652 cm^{-1} increases continuously with the growth of the H_2S amount adsorbed. Nevertheless, the intensity of these bands is low. The appearance of a band at 3652 cm^{-1} indicates that the first dose of H_2S leads to the formation of OH groups in the supercage of the zeolite. The band at 3696 cm^{-1} is attributed to the ν(OH) vibration of chemisorbed water. Indeed, a similar band at the same wavenumber is detected if only water (5 μmol $\cdot$ g^{-1}) is adsorbed on the NaY sample activated under the same conditions. Moreover, the appearance of water on the catalyst is confirmed by the presence of the δ(OH) band at 1641 cm^{-1} and a broad band at $\sim$3400 cm^{-1}. Formation of water after H_2S adsorption has been observed on metal oxides and has been attributed to dissociative H_2S adsorption and recombination with basic OH groups (20). However, since basic OH groups are not present in our zeolite, such an explanation cannot account for the formation of the water observed. Even with the drastic precautions we took, the presence of some traces of water in the cell could not be excluded. And it can be proposed that the introduction of H_2S displaces these traces toward the zeolite disk. It should be noted that, due to its high extinction coefficient, water is clearly observed on the amount detected, corresponding to less than 0.5% of the H_2S introduced.

In the 2750- to 2300-cm^{-1} zone that is characteristic of the stretching vibration of SH groups, various bands appear depending on the amount of H_2S introduced (Figs. 2 and 3). For the first dose of H_2S introduced, a small ν(SH) band at 2562 cm^{-1} is detected, which appears simultaneously with the OH band at 3652 cm^{-1}. The concomitant formation of SH groups with the zeolitic OH(HF) groups shows that a small amount of H_2S dissociates in the supercages of the NaY zeolite. The following equation can be proposed:

$$Na^+ + H_2S \rightarrow H^+ + Na^+SH^- \qquad \text{(mode 1)}.$$

When the higher amount of H_2S is adsorbed (NaY320), two small bands appear, at 2607 and 2574 cm^{-1} (shoulder) (Fig. 3). In a previous work (9), bands at 2608 and 2597 cm^{-1}, which arise simultaneously after H_2S adsorption at low temperature on silica, were attributed to antisymetric and symmetric vibrations of molecular H_2S. The similarities of the wavenumbers and the fact that the bands grow in parallel allowed us to attribute the bands at 2607 and 2574 cm^{-1} to antisymetric and symmetric vibrations of molecular H_2S coordinated to sodium cations (mode 2).

As soon as 70 μmol $\cdot$ g^{-1} of H_2S is introduced into the cell, the ν(SH) band presents a broad tail toward a lower wavenumber ($\sim$2525 cm^{-1}) (Fig. 3). Previous studies on adsorption of CH_3SH on alumina show that methanethiol species adsorbed through the H atom of the SH group are characterized by a low ν(SH) wavenumber ($\sim$2500 cm^{-1}). By analogy, we attribute the broad component situated at low value of our ν(SH) massif to H_2S H-bonded with the oxygen atom of the zeolite framework (mode 3). The spectra presented in Fig. 3 shows that the shape of the massif is not modified by the H_2S dose, contrary to what was observed previously on alumina. Thus, the intensity ratio between the bands at 2562 cm^{-1} and the tail at $\sim$2525 cm^{-1} shows that this latter mode of interaction is not predominant on NaY zeolite, even for the highest dose of H_2S introduced. This species does not correspond to H_2S in interaction with the OH groups created by H_2S dissociation or with the molecular H_2S coordinated to a sodium cation. Indeed, the intensity of the ν(OH) band as well as that of

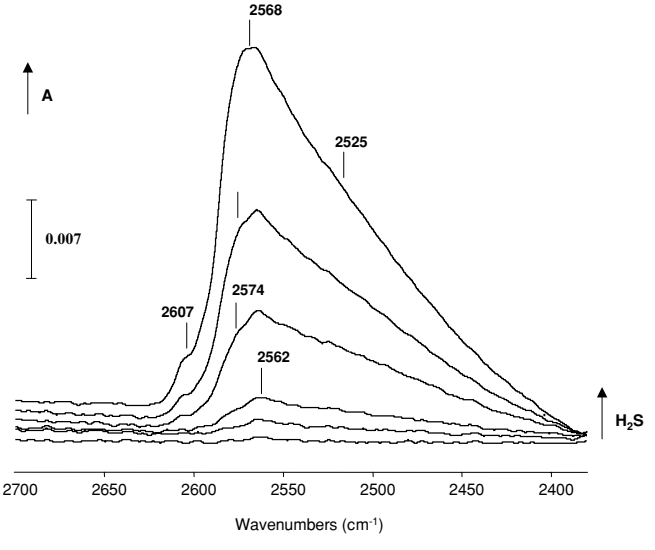

FIG. 3. Same spectra as in Fig. 2 but in the 2700- to 2400-cm^{-1} zone.

the ν(SH) shoulder at 2607 cm^{-1} is not modified when the amount of H-bonded H_2S increases. This confirms that the broad band around 2525 cm^{-1} corresponds to the H_2S H-bonded to the basic oxygen of the framework.

Evacuation at room temperature (RT) eliminates almost all of the SH bands except the very small band at 2562 cm^{-1} whereas no decrease of the intensity of OH bands at 3696 and 3652 cm^{-1} is observed. This phenomenon shows that pumping eliminates coordinatively and H-bonded H_2S species while species created by H_2S dissociation persists. This confirms that the small band at 2562 cm^{-1} characterizes Na^+SH^- species and it points out that the main part of the SH band at ~2568 cm^{-1} observed when a high amount of H_2S is introduced corresponds to molecular H_2S.

Figure 2 shows also the presence of a band at 2021 cm^{-1}. It is characteristic of COS, present as impurities in H_2S, likely adsorbed on cationic sites of NaY. For the highest H_2S doses, a band at 2070 cm^{-1} appears, indicating the presence of a COS gas phase in the IR cell.

The additional broad band at 3500–3000 cm^{-1}, which appeared when H_2S was added, is related to the presence of hydrogen bound between various water molecules or between zeolitic OH groups and adsorbed water. The presence of a "hole" in this broad massif at 3280 cm^{-1}can be noted. Since such a wavenumber coincides with the value of the harmonic of the water δ(OH) band, we propose that this spectral profile accounts for an Evans window. This feature has often been reported in the case of intermolecular interaction or in the case of H-bounded complexes (22–24). In our work, it is due to a Fermi resonance between the broad band of stretching vibrations of H-bonded water and the sharper harmonic of the water δ(OH) vibration.

Our results are very close to those reported by Karge and coworkers (12, 13). However, a sharp analysis of the spectra shows that some H_2S dissociation occurs for the first doses introduced on NaY. Moreover, we were able to detect a specific signal for coordinated H_2S. It could be noted that H_2S dissociation leads to the creation of some OH groups in the supercage only, although the diameter of the sixth O-ring of the entry of the sodalite cavity (4 Å) allows the H_2S molecule (3.6 Å) to enter. This points out the high basicity of a few of the oxygen atoms of the supercage.

Acidic Properties of the Activated Zeolite

The acidic properties of the NaY zeolite were characterized before H_2S introduction by pyridine (Fig. 4) and 2,6-dimethyl pyridine adsorption (Fig. 5).

The spectra of pyridine adsorbed on NaY did not present the IR bands at 1540 cm^{-1}, showing the absence of Brønsted acid centers on the evacuated sample, in agreement with the lack of zeolitic OH groups. Figure 4 shows bands at 1593 cm^{-1} and 1441 cm^{-1} that are specific of the ν_{8a} and ν_{19b} vibration modes of pyridine interacting with weak Lewis acidic sites. These coordination sites are attributed to the

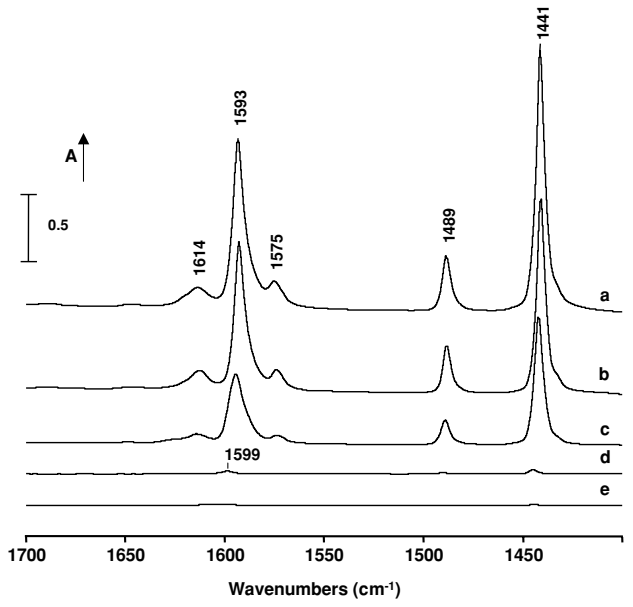

FIG. 4. IR spectra of pyridine adsorbed on NaY: (a) Pe, 4 mbars; (b–e) evacuation at RT and at 373, 473, and 523 K. (Difference spectra: after pyridine adsorption minus before).

cationic Na^+ centers. Moreover, a small band at 1614 cm^{-1} is observed. In a first interpretation, it could be attributed to Lewis acid sites presenting a rather strong acidic strength and could characterize the formation of an extraframework phase. However, pyridine evacuation at increasing temperatures does not show a preferential decrease in the intensity of the 1593-cm^{-1} band compared to that at 1614 cm^{-1}, as would be expected if these two bands characterized, respectively, weak and strong coordination sites. In the same way, the band at 1614 cm^{-1} is no longer detected after evacuation at 473 K while the band at 1593 cm^{-1} is still observed and is shifted to 1599 cm^{-1}. These results allow us to discard the attribution of the 1614-cm^{-1} band to strong Lewis acid sites. This conclusion is supported by other results of our group concerning the pyridine adsorption on calcium oxide, where such bands at ~1614 and ~1590 cm^{-1} were detected although CaO is known to present only very weak Lewis acid sites. The band at 1614 cm^{-1} more likely corresponds to a combination band since the presence of a ($\nu_1 + \nu_{6a}$) band at close wavenumbers was previously reported for liquid pyridine (25). Thus, if this band is clearly detected on NaY as well as on CaO, it is related to the fact that these two materials exhibit very weak coordination sites and therefore the low position of the ν_{8a} pyridine band allows more easily the distinguishing of the combination band at 1614 cm^{-1}.

Spectra recorded after DMP adsorption are presented in the 1700- to 1500-cm^{-1} zone, which is particularly interesting due to the occurrence of the bands of ν_{8a} and ν_{8b} vibrations, the most sensitive to the DMP adsorption mode.

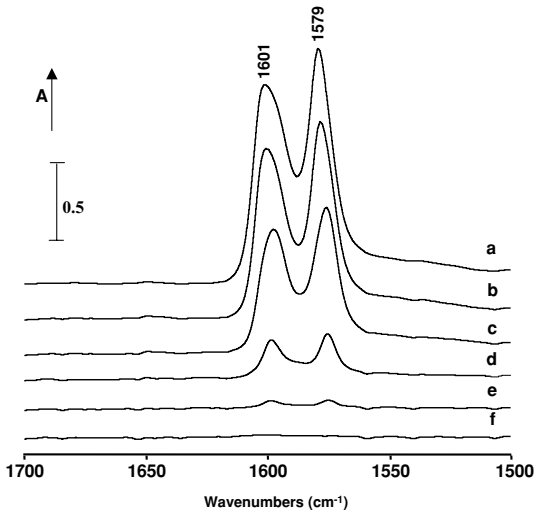

FIG. 5. IR spectra of 2,6-dimethylpyridine adsorbed on NaY: (a) Pe, 4 mbars; (b–f) evacuated at RT and at 373, 423, 473, and 523 K. (Difference spectra: after DMP adsorption minus before.)

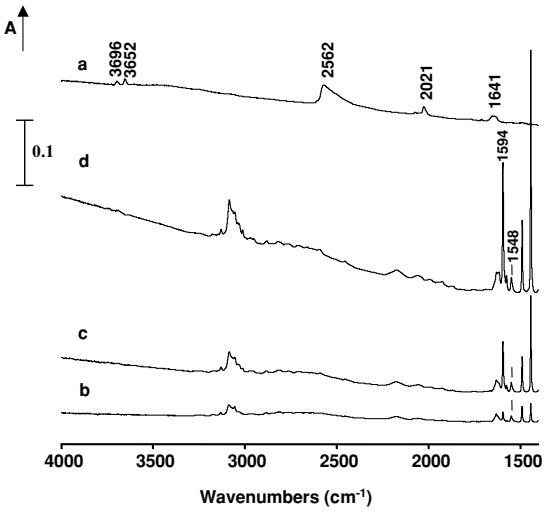

FIG. 6. Effect of pyridine introduction on the spectrum of H_2S adsorbed on NaY. (a) NaY1580 before pyridine adsorption (difference spectrum: after H_2S adsorption minus before); (b–d) after adsorption of 40, 122, and 244 μmol · g^{-1} of pyridine on NaY1580 (difference spectra: after pyridine adsorption minus before).

On NaY zeolite, DMP adsorption leads to the appearance of bands at 1601 and 1579 cm^{-1} (Fig. 5). Such bands indicate that DMP is weakly adsorbed evidently on cationic sodium sites, as observed with pyridine adsorption. We cannot exclude the possibility that some bands of DMP H-bonded to SiOH groups contribute to this massif, but taking into account the very small number of silanol groups, the main contribution comes from bands of DMP weakly coordinated. The absence of Brønsted acid sites is confirmed by the lack of bands between 1655 cm^{-1} and 1620 cm^{-1}, in agreement with the observation after the adsorption of pyridine. Moreover, no bands are detected around 1610 cm^{-1}, indicating that no Lewis acid centers presenting a rather strong acidity are present on the catalyst surface, in agreement with our previous interpretation of the pyridine results.

Effect of H_2S Adsorption on Acidic Properties

The effect of the introduction of 1580 μmol · g^{-1} of H_2S on the acidic properties of the NaY zeolite (NaY1580) were characterized by pyridine (Figs. 6 and 7) and 2,6-dimethylpyridine adsorption (Figs. 8 and 9).

Adsorption of increasing doses of pyridine on NaY samples with H_2S preadsorbed (NaY1580) leads to the appearance of bands characterizing the coordination of pyridine on the cationic centers (bands at 1594 and 1441 cm^{-1}) (Figs. 6 and 7). The number of coordinated species increases with the amount of pyridine introduced. However, the most interesting feature is the detection of small bands at 1629 and 1548 cm^{-1}, which provides evidence for the presence of protonated pyridine species (PyH^+) on the catalyst surface after contact with H_2S. These bands are clearly detected when small quantities of pyridine come into contact with the catalyst (Fig. 7, spectra a–c). In the presence of a higher amount of the adsorbate (4 mbars at equilibrium, spectra d), the intensities of the PyH^+ bands decrease although an expansion of the spectrum shows that a few of the protonated species are still present. This variation in pressure suggests that the main species responsible for the protonation of

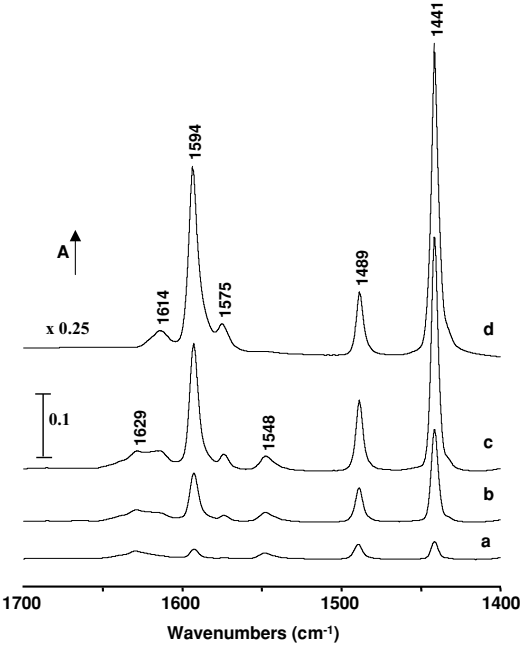

FIG. 7. IR spectra after the adsorption of (a) 40, (b) 122, and (c) 244 μmol · g^{-1} of pyridine; (d) Pe, 4 mbars on NaY1580. (Difference spectra: after pyridine adsorption minus before.) Spectra in the 1700- to 1400-cm^{-1} zone.

pyridine interacts weakly with the zeolite surface. The analysis of the 4000- to 3500-cm^{-1} zone does not show any modification in the intensity of the ν(OH) band of the zeolite or of water after an introduction of small doses of pyridine (Fig. 6, spectra b and c). This indicates that the Brønsted acid centers detected by the adsorption of pyridine do not originate from the OH groups formed via H_2S dissociation. It is notable that the perturbation of the OH bands at 3696 and 3652 cm^{-1} is only observed after introduction of 4 mbars at equilibrium of pyridine. Under these conditions, the small number of PyH^+ detected can evidently be related to the few zeolitic OH groups. It should be mentioned that, in presence of 4 mbars of pyridine, a strong decrease in the SH band at ~2568 cm^{-1} is also observed. The variation in the number of protonated species in parallel with the elimination of the main part of the molecular H_2S suggests that the protonation sites could be the molecular H_2S.

A similar experiment was performed with DMP (Figs. 8 and 9). The adsorption of increasing amounts of DMP on NaY1580 zeolite leads to the appearance of bands at 1601 and 1579 cm^{-1}, which were previously observed on the catalyst without H_2S (Fig. 9). A comparison of these spectra with those registered without preadsorption of H_2S indicates that the presence of H_2S leads to a small decrease in the number of coordinated DMP. This confirms that a part of the cationic sites are occupied by H_2S either in its molecular form or in its dissociated form as Na^+SH^- species. In agreement with the results obtained with pyridine, the interaction of H_2S with NaY leads to the creation of Brønsted acid

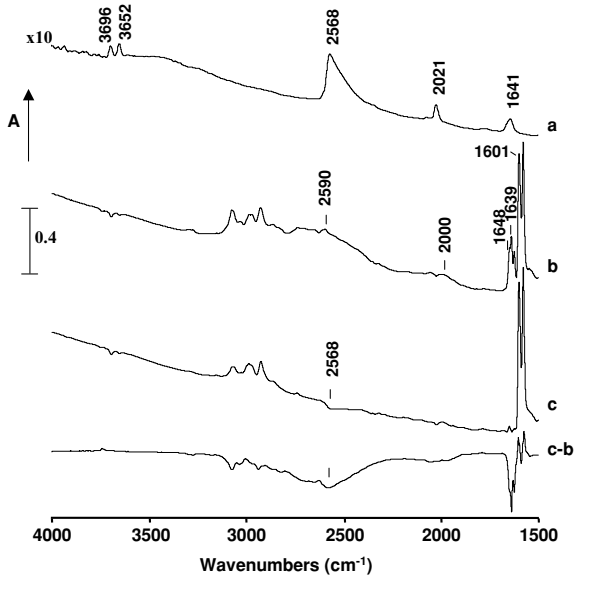

FIG. 8. Effect of 2,6-dimethylpyridine introduction on the spectrum of H_2S adsorbed on NaY. (a) NaY1580 before DMP adsorption (difference spectrum: after H_2S adsorption minus before); (b) after adsorption of DMP (Pe, 4 mbars) on NaY1580; and (c) after evacuation at RT (difference spectra: after DMP adsorption minus before).

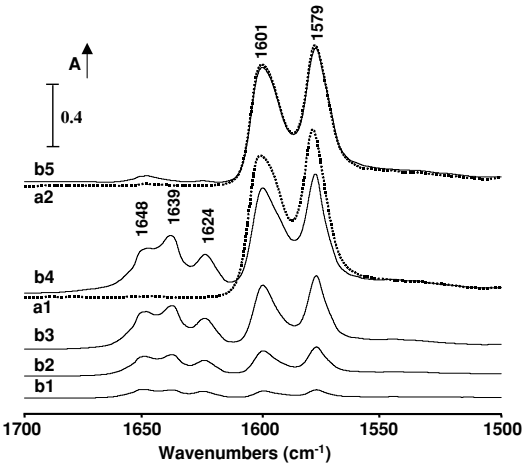

FIG. 9. Effect of H_2S adsorption on the IR spectra of 2,6-dimethylpyridine adsorbed. (a1, a2) DMP adsorption on pure NaY (dotted line): (a1) Pe, 4 mbars; and (a2) after evacuation at RT. (b1–b5) DMP adsorption on NaY1580 (solid line); (b1) 40 μmol · g^{-1}; (b2) 122 μmol · g^{-1}; (b3) 244 μmol · g^{-1}; (b4) Pe, 4 mbars; and (b5) after evacuation at RT. Spectra in the 1700- to 1500-cm^{-1} zone. (Difference spectra: after DMP adsorption minus before.)

centers, as revealed from the presence of the three bands, at 1648, 1639, and 1624 cm^{-1}. The intensity of these bands progressively increases when a higher amount of DMP is introduced into the cell. No decrease in the number of protonated species is observed when 3 Torr of DMP is in contact with the catalyst, the conversely of the phenomenon which occurred with pyridine.

The analysis of the zone above 1800 cm^{-1} shows, in addition to the bands at 3100–2800 cm^{-1} due to C–H bands of DMP, the presence of two broad bands centered close to 2590 and 2000 cm^{-1} (Fig. 8), the intensities of which increase with an increasing amount of DMP introduced. Taking into account a previous study on zeolite (24), one can interpret these broad bands separated by a hole at 2200 cm^{-1} as Fermi resonance between ν(NH) and a combination δ(NH) + γ(NH) band. Thus, the occurrence of this resonance confirms the formation of protonated DMP species.

Evacuation at room temperature of the NaY1580 after its contact with 4 mbars of DMP leads to significant modification of the spectrum (Figs. 8 and 9). To analyze more clearly these transformation the difference between the spectrum taken after evacuation of the NaY1580 with 4 mbars of DMP minus the spectrum registered before the evacuation is exhibited (Fig. 8, spectrum c-b). The most striking point is that evacuation leads to an almost complete elimination of $DMPH^+$ species since the bands at 1648, 1638, and 1624 cm^{-1} almost completely disappear, in agreement with the disappearance of broad bands at 2590 and 2000 cm^{-1}. The ν_8 bands which remain present a very low intensity and are observed at 1650 and 1624 cm^{-1}. As already noted

with pyridine, the small $DMPH^+$ band, which remains after evacuation, can be related to the small number of zeolitic OH groups, in agreement with the wavenumbers which coincide with those reported for DMP adsorption on HY zeolite (26).

Additionally, evacuation of DMP coadsorbed with H_2S results in the elimination of the main part of the SH species (Fig. 8 spectrum c-b: negative band at ~2568 cm^{-1}). The difference spectrum provides also an evidence for a general decrease in the number of DMP molecules interacting with the surface, since the intensity of the C–H band at 3200–2800 cm^{-1} decreases, although an increase in the bands in the 1600- to 1575-cm^{-1} range is noted after evacuation. This likely indicates a transformation of some physisorbed DMP species into coordinated ones. Such a feature has already being observed after evacuation of a large amount of probe molecule adsorbed at RT or lower temperature on the zeolite. It could be explained by a better accessibility of pore sites after elimination of some physisorbed species.

Therefore, the question which arises is which species are responsible for the protonation of DMP in the presence of H_2S. To answer this query, we determined which species no longer interact with DMP after evacuation of the NaY1580 sample.

In the 4000- to 3500-cm^{-1} zone (Fig. 10), the presence of 4 mbars of DMP leads to the perturbation of three ν(OH) bands, at 3745 (SiOH), 3696 (H_2O), and 3652 cm^{-1} ((OH)HF) . RT evacuation removes DMP molecules which were interacting with SiOH groups. Thus, the SiO–H band at 3750 cm^{-1} appears as a positive band on the difference spectrum presented in Fig. 10 (spectrum b-a). However, evacuation at RT does not induce any modification of the OH bands at 3696 and 3652 cm^{-1}, which evidently indicates that the hydroxyl groups corresponding to the traces of water adsorbed on the zeolite and to the zeolitic OH groups formed by H_2S dissociation are still in interaction with DMP. Previous studies show that silanol groups only interact by H-bonding with DMP since they are not acidic enough to protonate DMP (9). Therefore, the removal of the interaction between DMP and SiOH cannot explain the elimination of $DMPH^+$ species by evacuation at RT. Moreover, the decrease in the number of $DMPH^+$ species cannot be related to an elimination of water since the intensity of the 3696 cm^{-1} band is not reduced by pumping. This feature points out that the traces of water are not responsible for the main part of the Brønsted acidity.

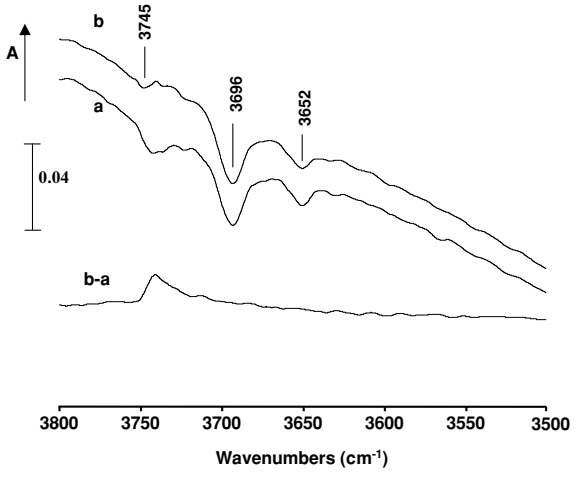

FIG. 10. Spectra in the ν(OH) vibration zone of the effect of 2,6-dimethylpyridine introduction on the spectrum of NaY1580. (a) After adsorption of DMP (Pe, 4 mbars); (b) after evacuation at RT (difference spectra: in presence of DMP minus before DMP adsorption).

The analysis of the 2700- to 2500-cm^{-1} zone (Fig. 8) shows on spectrum c and more clearly on difference spectrum (c-b) that evacuation leads to the elimination of some SH species since the ν(SH) band at ~2574 cm^{-1} clearly decreases. Therefore, a relationship between the presence of molecular H_2S and the formation of protonated DMP species as well as of pyridinium species appears. This result allows us to propose that the interaction of H_2S with the cationic Na^+ centers could induce a perturbation in the electronic bond in the H_2S molecule and leads to the appearance of a positive charge on the hydrogen atom in the molecule, which becomes able to protonate DMP and pyridine. The increase in the acidity of the hydroxyl group of alcohols by their coordination on Lewis acid centers such as $SbCl_5$ was previously reported in the literature (27–29). To our knowledge, such an increase in acidity by coordination of a reactant or by a product of a reaction with the surface of a solid catalyst has not been reported in the literature.

The weak interaction of H_2S with Na^+, previously evidenced, explains why pumping at RT, which eliminates coordinated H_2S, also leads to a decrease in the number of protonated DMP species. Experiments with pyridine adsorption also indicate that species responsible for the protonation weakly interact with the zeolite. Indeed, the decrease in the number of pyridinium species detected when large amounts of pyridine were introduced into the cell can be explained by a competitive adsorption between molecular H_2S and pyridine on Na^+ cations. With DMP, the presence of methyl groups reduces the strength of the coordination. Therefore, for the same equilibrium pressure, DMP, which interacts less strongly with cationic sites, does not displace coordinated H_2S while pyridine displaces it.

In the presence of H_2S, DMP provides evidence for the presence of protonic sites, with these sites being characterize by the appearance of three distinct bands, at 1624, 1639, and 1648 cm^{-1}. From previous studies (9, 10, 26, 30–32) it appears that whatever the nature of the sample, a band always appears at a wavenumber close to 1624 cm^{-1} when $DMPH^+$ is formed. This band characterizes the ν_{8b} vibration of protonated DMP species. Conversely, the position of the ν_{8a} vibration of $DMPH^+$ is sensitive to the environment

and the strength of the protonic sites since it has been previously detected between 1655 and 1630 cm^{-1}. In the present work, two distinct ν_{8a} bands can be evidenced, at 1648 and 1639 cm^{-1}. They could be related to the coordination of H_2S with sodium cations localized in different positions or cavities.

CONCLUSION

The effect of H_2S adsorption on the acidic properties of NaY zeolite was studied by IR spectroscopy using pyridine and 2,6-dimethylpyridine as probe molecule. The Na^+ sites present a weak Lewis acid character. The number of accessible cations decreases in the presence of H_2S, likely due to the existence of molecular H_2S coordinated to Na^+ sites or to the dissociation of a low number of H_2S, which leads to the formation of OH and Na–SH species. Both probe molecules (pyridine and 2,6-dimethylpyridine) detect, in presence of H_2S, the appearance of Brønsted acid sites and provide evidence for the removal of these sites after evacuation at RT. Our results point out that this elimination of pyridinium and lutidinium species does not lead to a modification in the intensity of the ν(OH) bands. Conversely, a relationship is established between the presence of molecular H_2S coordinated to cationic Na^+ sites and the formation of protonated species. From these results, we can propose that coordination of H_2S on cationic sites modifies the electronic distribution in the molecule of hydrogen sulfide and therefore changes the polarity of the SH bond. This leads to the appearance of a positive charge on the H atom of the molecular H_2S, which, then, presents a proton-donating ability. These observations suggest the existence of a relationship between the acidity of the cation in the zeolite and the acidity induced on the adsorbate. This study shows that reactants or products of the reaction even in their molecular forms can modify the surface acidity of the catalyst. Moreover, it points out that an adsorbate in just weak interaction with the surface can modify acid–base properties and thus can become a potential active site. Therefore, it underlines the importance of characterizing surface properties under conditions as close as possible to the reaction conditions.

REFERENCES

1. Pieplu, A., Saur, O., and Lavalley, J. C., *Catal. Rev.–Sci. Eng.* **40**, 409 (1998).
2. Maskina, A. V., *Russ. Chem. Rev.* **64**, 1131 (1995).
3. Ziolek, M., and Bresinska, I., *Zeolites* **5**, 245 (1985).
4. Ziolek, M., Nowinska, K., and Leksowska, K., *Zeolites* **12**, 710 (1992).
5. Ziolek, M., Czyzniewska, J., Lamotte, J., and Lavalley, J. C., *Zeolites* **16**, 42 (1996).
6. Ono, Y., *Stud. Surf. Sci. Catal.* **5**, 19 (1980).
7. Hölderich, W. F., Hesse, M., and Naümann, F., *Angew. Chem.* **27**, 226 (1988).
8. Van Gestel, J., Finot, L., Leglise, J., and Duchet, J.-C., *Bull. Soc. Belg.* **189**, 4 (1995).
9. Petit, C., Maugé, F., and Lavalley, J. C., *Stud. Surf. Sci. Catal.* **106**, 157 (1997).
10. Travert, A., and Maugé, F., *Stud. Surf. Sci. Catal.* **127**, 269 (1999).
11. Travert, A., Manoilova, O. V., Tsyganenko, A. A., Maugé, F., and Lavalley, J. C. *J. Phys. Chem. B* **106**, 1350 (2002).
12. Karge, H. G., and Rasko, G. J., *J. Colloid Interface Sci.* **64**, 522 (1978).
13. Karge, H. G., Ziolek, M., and Laniecki, M., *Zeolites* **7**, 197 (1987).
14. Forster, H., and Schuldt, M., *J. Colloid Interface Sci.* **52**(2), 380 (1975).
15. Hosotsubo, T., Sugioka, M., and Aomura, K., *Bull. Fac. Eng. Hokkaido Univ.* N102 (1981).
16. Lahousse, C., Aboulayt, A., Maugé, F., Bachelier, J., and Lavalley, J. C., *J. Mol. Catal.* **84**, 283 (1993).
17. Jacobs, P. A., and Heylen., C. F., *J. Catal.* **34**, 267 (1974).
18. Mattulewicz, E. R. A., Kerkhof, F. P. J. M., Mouljin, L. A., and Reitsma, H. J., *J. Colloid Interface Sci.* **77**, 110 (1980).
19. Corma, A., Rodella, C., and Fornest, V., *J. Catal.* **88**, 374 (1984).
20. Datta, A. G., and Cavell, R., *J. Phys. Chem.* **89**, 450 (1985).
21. Saur, O., Chevreau, T., Lamotte, J., Travert, J., and Lavalley, J. C., *J. Chem. Soc., Faraday Trans. 1* **77**, 427 (1987).
22. Evans, J. C., *Spectrochim. Acta* **16**, 994 (1960).
23. Bratos, S., and Ratajczak, H., *J. Chem. Phys.* **76** (1), 77 (1982).
24. Lavalley, J. C., Anquetil, R., Czyzniewska, J., and Ziolek, M., *J. Chem. Soc., Faraday Trans.* **92**, 1263 (1996).
25. Sidorov, A. N., *Opt. Spektrosk.* **8**, 51 (1960).
26. Jolly, S., Saussey, J., and Lavalley, J. C., *J. Mol. Catal.* **86**, 401 (1994).
27. Gallas, J. P., and Binet, C., *Adv. Mol. Relax. Interact. Process.* **24**, 191 (1982).
28. Taillandier, M., Tochon, G., and Taillandier, E., *J. Mol. Struct.* **10**, 471 (1971).
29. Derouault, G., Dziembowska, T., and Forel, M. T., *Spectrochim. Acta Part A* **35**, 773 (1979).
30. Clet, G., Goupil, J. M., and Cornet, D., *Bull. Soc. Chim.* **134**, 223 (1997).
31. Lahousse, C., Maugé, F., Bachelier, J., and Lavalley, J. C., *J. Chem. Soc., Faraday Trans.* **91**, 2907 (1995).
32. Travert, A., Ph.D. thesis. University of Caen, 2000.